Environmental Research 217 (2023) 114951

Contents lists available at ScienceDirect

Environmental Research

journal homepage: www.elsevier.com/locate/envres

Characterizing the efficiency of low-cost LED lights for conducting laboratory studies to investigate polycyclic aromatic hydrocarbon photodegradation processes

Marieh Arekhi, Leigh G. Terry, T. Prabhakar Clement *

Department of Civil, Construction and Environmental Engineering, The University of Alabama, Tuscaloosa, AL, USA

ARTICLE INFO

Keywords:
PAHs
Photodegradation
LED light
UV-A light
High molecular weight PAHs
First-order kinetics

ABSTRACT

Polycyclic aromatic hydrocarbons (PAHs) are common contaminants ubiquitously present in various waste products such as biosolids (e.g. wastewater sludges), oil spill residues (e.g. tarballs), road asphalts, and combustion byproducts. In this study, the photodegradation of PAHs is investigated under natural sunlight (cloudy and sunny/clear weather conditions), and using two types of artificial LED light sources. This is the first study to investigate the relative efficiency of low-cost LED light sources for conducting laboratory-scale PAH photodegradation experiments and directly comparing the results against those obtained using natural sunlight. Two types of LED light sources are investigated in this study: a light source with a full-spectrum range (380 nm–780 nm) that can cover the broad wavelength range of solar light reaching the Earth's surface, and a light source with a UV-A range (365 nm) that covers the UV range of the solar spectrum reaching the Earth's surface. The results show that the degradation of high molecular weight (HMW) PAHs is primarily due to photodegradation, and other lighter PAHs are degraded by both photodegradation and evaporation processes. HMW PAH photodegradation reactions follow the first-order degradation kinetics. The degradation rate constants of different PAHs are used to compare the relative efficiency of the light sources. The data show that the full-spectrum LED induced PAH photodegradation rates are similar to the natural sunlight induced rates. Furthermore, when the values of the rate constants are normalized to respective irradiance levels, the normalized rates for HMW PAH photodegradation under both full-spectrum LED light and natural sunlight are almost identical. However, the normalized photodegradation rate constants of HMW PAHs under the UV-A LED light are about two to three orders of magnitude higher than the sunlight as well as the full-spectrum-LED values. Therefore, the UV-A LED light is the optimal low-cost light source for studying PAH photodegradation processes under laboratory conditions.

1. Introduction

Polycyclic aromatic hydrocarbons (PAHs), a group of organic compounds with two or more fused aromatic rings, are common contaminants ubiquitously present in the environment (Chen et al., 2003; Li et al., 2021). PAHs, especially those with four or more rings, are considered hazardous pollutants due to their genotoxicity, mutagenicity, and carcinogenicity (Li et al., 2021; Vela et al., 2012). Several environmental agencies including the United States Environmental Protection Agency (USEPA) and European Union have classified several PAHs as compounds that pose significant human health risks (Vela et al., 2012; Yang et al., 2018). Because of their hydrophobicity and low solubility, high molecular weight PAHs tend to sorb to particulates and hence are widely transported through the environmental system and can remain in the environment for several years (Arekhi et al., 2020; Gustitus and Clement, 2017). Consequently, PAHs pose a considerable hazard not only to human populations living in urban areas, but also to natural ecosystems (Marquès et al., 2017).

PAHs may enter the environment from natural sources such as biomass, plant synthesis, organic matter diagenesis, and forest fires; and anthropogenic sources such as waste sludges, industrial wastes, oil spills from crude and refined petroleum products, residential heating, power generation, incineration, automobiles, and asphalt roads (Clement and John, 2022; Marquès et al., 2017). Human activities, e.g. wastewater

* Corresponding author.
E-mail address: pclement@ua.edu (T.P. Clement).

https://doi.org/10.1016/j.envres.2022.114951
Received 19 September 2022; Received in revised form 19 November 2022; Accepted 24 November 2022
Available online 25 November 2022

treatment plants, biowaste incinerators, and oil spills, are the main contributor that distributes PAHs into air, soil, sediment, and water environments (Chen et al., 2003; Li et al., 2021; Pizzini et al., 2022). PAH pollution is ubiquitously present in various areas including industrial zones, commercial ports, agriculture areas, oil and gas exploitation zones, small tourist towns, and megacities (Dai et al., 2022). Since PAHs are distributed over a broad area, the management of PAH pollution remains as a major challenge.

PAHs may undergo various natural transformation processes in the environment such as biodegradation, chemical transformation, and photodegradation (John et al., 2016). It has been well established that photodegradation plays a significant role in degrading PAHs when they are exposed to sunlight (Aeppli, 2022; Radović et al., 2014; Sharpless et al., 2016). For example, John et al. (2016) showed that PAHs in the Deepwater Horizon (DWH) oil spill residues weathered significantly when the oil spill residues floating over the Gulf of Mexico were re-exposed to sunlight. Photodegradation typically serves as an initial step in enhancing bioavailability and facilitating further biodegradation of PAHs (King et al., 2014; Mambwe et al., 2021).

Photodegradation research studies can be conducted under natural sunlight or artificial light (Marquès et al., 2017). Natural sunlight is not preferable for fundamental investigations due to various uncontrollable factors such as intensity variations and the variations in the spectral distribution of solar radiation (Esen et al., 2017). Artificial lights are preferred since they allow investigators to conduct laboratory-scale photodegradation studies in a controlled setting, and hence can provide reproducible and reliable results (Esen et al., 2017). Artificial lights to be used for photodegradation studies should, however, mimic the natural characteristics of sunlight, especially the spectral distribution and irradiance level. Typical solar irradiance reaching the earth is ~1367 W/m^2 at the upper atmosphere, diminishing to ~1120 W/m^2 at the ground level, as determined by the World Meteorological Organization (Shankar et al., 2015). The relevant wavelengths of solar light reaching the earth range from 100 nm to 1 mm and consist primarily of UV, visible, and infrared (IR) radiation with relative energy distribution of ~5%, 43%, and 52%, respectively. The UV spectrum is further classified into UV-A (315–400 nm), UV-B (280–315 nm), and UV-C (100–280 nm) regions. The UV-C and UV-B radiations are mostly absorbed by the earth's atmosphere; therefore, the UV radiation reaching the earth's surface consists of 95% UV-A, 5% UV-B, and almost 0% UV-C (Shankar et al., 2015).

Several laboratory-scale PAH photodegradation studies have been conducted using various types of artificial lights with limited wavelength ranges or limited intensity. Unfortunately, most studies do not provide information about the spectrum and irradiance level of the lamp used (Gupta and Gupta, 2015; Zhang et al. 2006, 2008, 2010). For example, Marquès et al. (2016b) investigated the photodegradation of PAHs in soils spiked with 16 USEPA priority PAHs using the Binder KBWF 240 climate chamber with fluorescent lamps, the spectrum of the lamps was not specified, and the light intensity was 9.6 W/m^2. The study found that the photodegradation rates of PAHs were dependent on exposure time, the molecular weight of hydrocarbons, and soil texture. In another research, Marquès et al. (2017) showed that PAHs' photodegradation rates were higher under solar radiation than under the Binder KBWF 240 climate chamber with fluorescent lamps. Since the spectrum of the lamp used was not specified in this study, it is not clear why solar radiation could result in higher photodegradation levels of PAHs compared to the fluorescent lamp.

Gas-discharge lamps including xenon arc, metal halide, mercury, mercury-xenon, and fluorescent UV lamps have been used in photodegradation studies (Shankar et al., 2015). However, these lamps have technical problems including inconsistency in the spectral distribution from one lamp to another of the same type, the need for warm-up and cool-down steps, the need for careful maintenance, limited lifetime, high power consumption, high heat load, thermal management issues, complicated controls, and most importantly the lamps are expensive (López-Fraguas et al., 2019; Shankar et al., 2015; Tavakoli et al., 2021). In contrast, light-emitting diodes (LEDs) have several advantages including low cost, low power consumption, long lamp life, instant on-off function, yield a wide range of spectrum, and they employ environmentally friendly manufacturing technologies when compared to other traditional lamps (Subramanian and Prakash, 2021; Yu et al., 2019). Freeman and Ward (2022) used a custom-built LED reactor system to investigate the effect of the light spectrum on the photo-dissolution of Macondo crude oil and reported that oil photo-dissolution decreases exponentially with increasing the wavelength. In another study, Song et al. (2016) demonstrated that newly emerging UV-LEDs provide a promising alternative for water disinfection and offer many advantages such as multiple wavelengths, adjustable radiation patterns, and are more effective in inactivating microorganisms over traditional mercury lamps. Thus, over the past decade, LED-based light sources have been used as a substitute for gas-discharge lamps in several applications (López-Fraguas et al., 2019). Typically, LEDs are known to have operating lifetimes that are over an order of magnitude greater than those of xenon lamps (Linden et al., 2014). Therefore, a LED lamp is an economic and safe alternative to traditional lamps (Ullah et al., 2020). However, to the best of our knowledge, no one has characterized the efficiency of various LED light sources when they are used as an alternative to natural sunlight for studying PAH photodegradation processes.

The objective of this study is to characterize the efficiency of two types of low-cost LED light sources (full-spectrum and UV-A lights) for conducting laboratory-scale PAH photodegradation investigations. The following two research hypotheses are tested in this study: 1) the full-spectrum LED-light induced photodegradation rates of PAHs are similar to the natural sunlight induced photodegradation rates when the rates are scaled to the irradiance levels; and 2) a light source with the UV-A wavelength range can substantially accelerate PAH photodegradation rates. The UV-A light was selected since the solar spectrum that reaches the earth's surface primarily includes the UV-A range (Shankar et al., 2015). The photodegradation rates of 16 USEPA priority PAHs were investigated at two different initial concentrations (100 ppb and 1000 ppb) using full-spectrum and UV-A lights under laboratory conditions, and natural sunlight under two types of field conditions (cloudy, and sunny which is referred to as clear conditions henceforth). The hypotheses are tested by comparing the LED light results against the results obtained under natural sunlight.

2. Materials and methods

2.1. Materials

The solvents (hexane, dichloromethane (DCM), methanol, and acetone, all HPLC grade) were purchased from VWR International Company (Suwanee, GA, USA). A PAH standard mixture consisting of 16 USEPA PAHs (naphthalene, acenaphthylene, acenaphthene, fluorene, phenanthrene, anthracene, fluoranthene, pyrene, benzo [*a*]anthracene, chrysene, benzo [*b*]fluoranthene, benzo [*k*]fluoranthene, benzo [*a*]pyrene, dibenz [*a,h*]anthracene, indeno [*1,2,3,-cd*]pyrene, and benzo [*ghi*]perylene) was purchased from Sigma-Aldrich (St. Louis, MO, USA). A mixture of deuterated PAHs consisting of acenaphthene-d_{10}, phenanthrene-d_{10}, chrysene-d_{12}, and perylene-d_{12} was used as a surrogate standard and was purchased from Agilent Technologies (Wilmington, DE, USA). An internal standard *p*-terphenyl-d_{14} (purity >98.5%) was purchased from AccuStandard (New Haven, CT, USA). Glass petri-dishes (with lid, soda-lime glass, dish H 12 mm, diam. 40 mm) were purchased from Sigma-Aldrich (St. Louis, MO, USA). GC capillary column (J&W DB-EUPAH, 60 m × 0.250 mm × 0.25 μm, p/n 122-96L2) and deactivated GC liners (splitless tapered glass wool) were purchased from Agilent Technologies (Wilmington, DE USA).

Artificial light sources used in this study were BESTVA DC series 4000 W full-spectrum LED lamp (Fig. S1–a, referred to as the full-

Table 1
Gas chromatograph (GC) and mass spectrometer (MS) parameters.

GC conditions	
Inlet temperature	320 °C
Inlet pressure	21.186 psi
Carrier gas	Helium
Flow rate	1.2 ml/min
Injection mode	Pulsed splitless
Oven program	50 °C (0 min hold); 60 °C/min to 180 °C (0 min hold); 10 °C/min to 230 °C (1 min hold); 35 °C/min to 330 °C (25 min hold) Post-run: 335 °C (6 min hold)
Total run time	42 min
Injection volume	1 μl
Transfer line temperature	325 °C
MS conditions	
Delta EMV	−70 eV
Acquisition parameters	Electron Ionization (EI)
Solvent delay	5 min
MS source temperature	320 °C
Quadrupole temperatures	150 °C

spectrum LED light henceforth) and Somesino 300 W UV-A LED lamp (Fig. S1–b, referred to as the UV-A LED light henceforth); they were purchased from Amazon for $359 and $133, respectively. The traditional solar simulators, typically used for photodegradation studies, would cost about $10,000 to $20,000. The full-spectrum LED light provided a wavelength range of 380 nm–780 nm (Fig. S1–c), and the UV-A LED light provided a single wavelength of 365 nm (Fig. S1–d). SM206 digital solar power meter to record irradiance levels of the lights and a temperature/humidity meter were purchased from Amazon. A clear acrylic OP-3 UV filtering sheet to filter out UV light from the light sources was purchased from TAP Plastics.

2.2. Sample preparation and experimental design

The 16 USEPA PAH standard mixture (with the stock solution concentration of 0.2 mg/ml) was serially diluted with hexane:DCM solvent mixture (50%, v/v, referred to as HD henceforth) to the concentrations of 1000 ng/ml or ppb (referred to as ppb henceforth) and 100 ppb with the final volumes of 50 ml for each. Then, exactly 1 ml of the prepared solutions (1000 ppb and 100 ppb PAHs) were transferred to petri-dishes. The samples were kept under the fume hood for several minutes to allow the solvent to evaporate, the fume hood light was turned off to avoid any possible photodegradation. The samples were then exposed to natural sunlight and LED light irradiation. The irradiation was measured by the SM206 digital solar power meter. During irradiation, the samples were exposed to direct light with uncovered petri-dishes, and the control samples were covered with aluminum foil to prevent exposure to irradiation. For the UV filtering experiments, all irradiated and control samples were covered with the clear acrylic OP-3 UV filtering sheet. The total irradiation time was 24 h, with samples taken at 0, 1, 4, 8, and 24 h time points. All the samples were prepared in duplicate.

The natural sunlight experiments were exposed to 8 h of irradiation each day (10 am to 6 pm during the period of April to August 2022); thus, each experiment was conducted over 3 full days. The sunlight experiments were conducted under two different weather conditions. The first experiment was performed during cloudy conditions with an average solar irradiance of 600 W/m^2 (ranging from 300 to 1000 W/m^2 during the day, see Table S1). The second experiment was performed during clear conditions with an average solar irradiance of 1200 W/m^2 (ranging from 900 to 1300 W/m^2 during the day with the highest irradiance level detected around noon, see Table S2). The outdoor temperature ranged from 22 to 30 °C during cloudy conditions and 30–34 °C during clear conditions with the high temperature detected around noon, and the average temperatures were 27 °C and 33 °C, respectively. The laboratory temperature was around 22 °C. The full-spectrum LED light was set up at two different heights of 40 cm and 10 cm from the samples yielding two irradiance levels of 600 W/m^2 and 1200 W/m^2, respectively, recorded by the SM206 digital solar power meter. The UV-A LED light was set up at the height of 10 cm and yielded an irradiance level of 4 W/m^2.

2.3. Sample extraction

The irradiated and control samples were spiked with 20 μl of 50 μg/ml surrogate standards in petri-dishes and then washed with HD solvent to extract the PAHs. The dishes were sequentially extracted with 10 × 1 ml of HD. The extracts were concentrated under a gentle stream of nitrogen to adjust the final volumes to 1 ml and were spiked with 10 μl of 50 μg/ml *p*-terphenyl-d_{14} as an internal standard, before chemical analysis.

2.4. GC/MS analyses

The samples were analyzed using an Agilent 7890 B gas chromatograph (GC) coupled to an Agilent 7000C triple quadrupole mass spectrometer (MS) using a SIM (single ion monitoring) method (see Table 1 for the method parameters). The method used was similar to the previously published analytical approach (Han et al., 2020; John et al., 2016). The separation of the various compounds was achieved using an Agilent J&W DB-EUPAH column, and helium as the carrier gas.

2.5. Identification and quantification of target compounds

The target PAH compounds were identified by their characteristic mass-to-charge ratios (*m/z*) listed in Table S3, and the peak areas were integrated using Agilent Technologies MassHunter MS quantification software (version B.09.00) to quantify the concentrations. The chromatographic peak areas of the internal standard *p*-terphenyl-d_{14} were used to normalize the PAHs' chromatographic peak areas.

The quantification process was based on the calibration curves generated using the PAH standard mixture consisting of 16 PAHs (Table S3). Six calibration points at concentration levels of 1, 5, 10, 50, 100, and 200 ppb spiked with the internal standard (*p*-terphenyl-d_{14}, 500 ppb) were used to quantify the samples with initial concentrations of 100 ppb PAHs. Eight calibration points at concentration levels of 1, 5, 10, 50, 100, 200, 500, and 1000 ppb spiked with the internal standard (*p*-terphenyl-d_{14}, 500 ppb) were used to quantify the samples with initial concentrations of 1000 ppb PAHs.

The calibration responses were linear across the selected analytical range, yielding correlation coefficient (R^2) values of 0.95 or greater. An inverse concentration weighting method was used to minimize bias from low-concentration calibration points for the compounds with low concentrations. The retention time of each chromatogram of the target compounds was set within ±60 s relative to the shift of the internal standard. Background correction and baseline stabilization were performed by running solvent blanks.

2.6. Determination of photodegradation rates and net degradation levels

The first-order photodegradation rate constant of various PAH compounds in the irradiated samples was calculated using the following equation:

$$C_t = C_0\, e^{-kt} \quad (1)$$

where k is the first-order photodegradation rate constant [T^{-1}], and C_t and C_0 are the concentrations of the PAHs in the irradiated sample at any time "t" and the original sample at t = 0, respectively. In this study, all

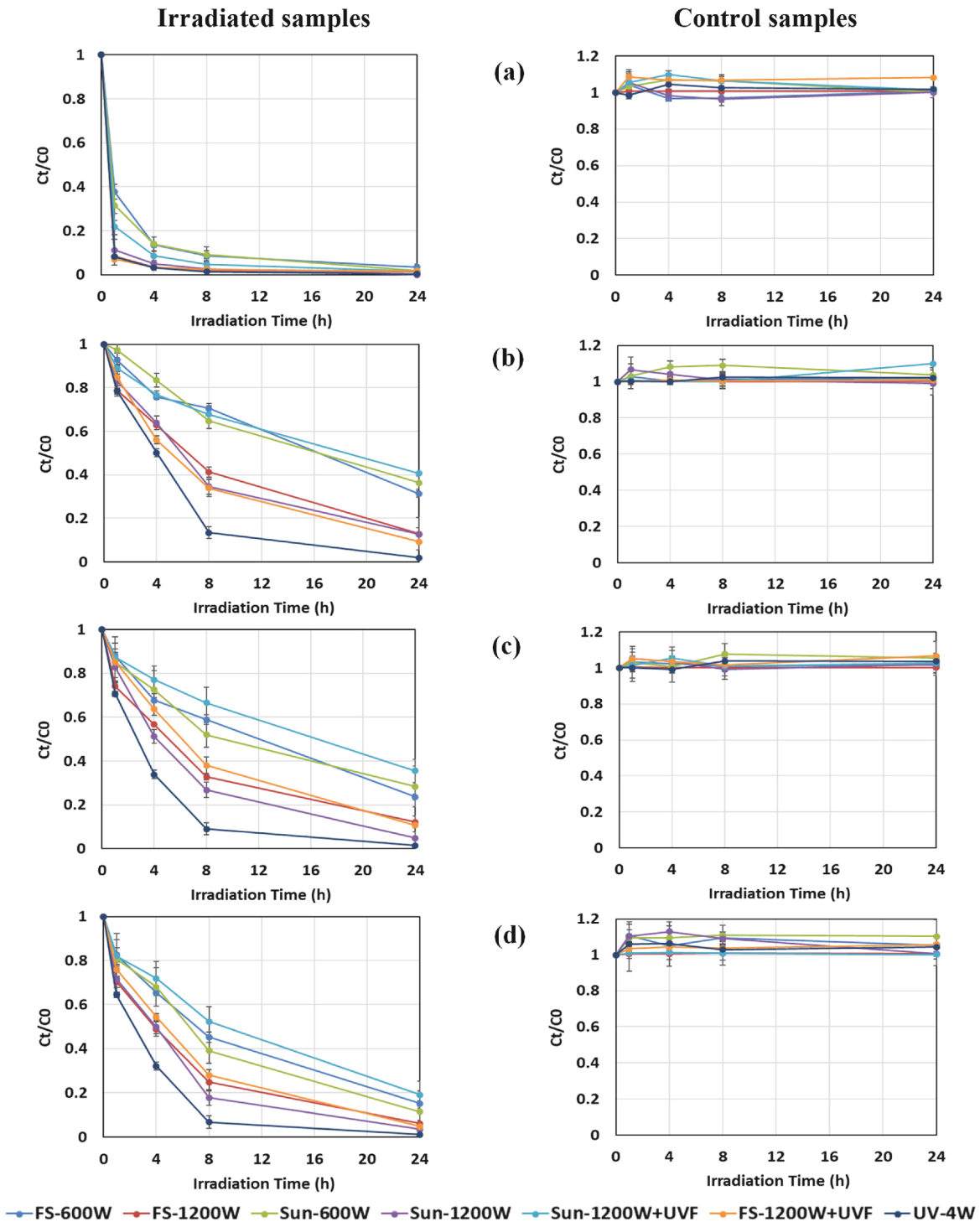

Fig. 1. Changes in the concentrations of HMW PAHs with irradiation time under full-spectrum LED light at two irradiance levels (FS–600 W and FS-1200W), sunlight during cloudy (Sun-600 W) and clear (Sun-1200 W) conditions, clear sunlight with a UV filter (Sun-1200 W+UVF), full-spectrum LED light with a UV filter (FS–1200 W+UVF), and UV-A LED light (UV–4W). a) benzo [*a*]anthracene, b) chrysene, c) benzo [*b*]fluoranthene, and d) benzo [*k*]fluoranthene. The initial concentration of the samples was 1000 ppb.

the k values are reported in the unit of [hour^{-1}], referred to as [h^{-1}] henceforth, and all the concentration values are reported in the unit of [ppb].

A new irradiation-normalized first-order photodegradation rate constant (k_n) is defined for the PAH compounds in this study using the following equation:

$$K_n\left(\frac{h^{-1}}{W/m^2}\right) = \frac{K\left(h^{-1}\right)}{Irradiance\ level(W/m^2)} \quad (2)$$

where "*irradiance level*" is the flux rate of irradiance from the light source measured in [W/m^2]. The k_n values are scaled as kilo-watts of energy (kW) and are reported as $\left[\frac{h^{-1}}{kW/m^2}\right]$ in this study.

The net degradation level (DL) percentage of PAH compounds in the

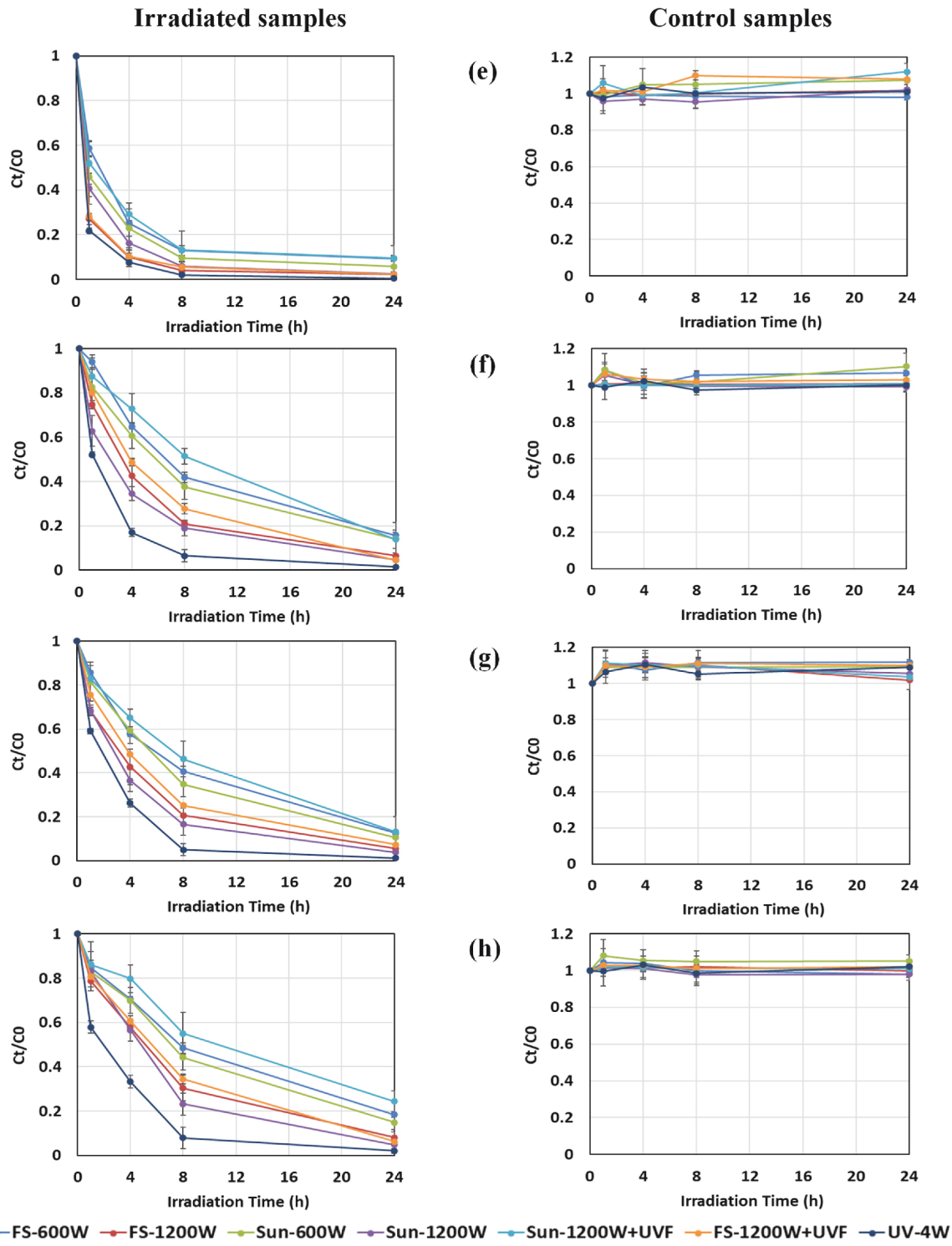

Fig. 2. Changes in the concentrations of HMW PAHs with irradiation time under various conditions (as explained in Fig. 1 caption). e) benzo [*a*]pyrene, f) dibenz [*a, h*]anthracene, g) indeno [*1,2,3-cd*]pyrene, and h) benzo [*ghi*]perylene. The initial concentration of the samples was 1000 ppb.

irradiated samples at any given time "t" was calculated using the following equation:

$$DL(\%) = \left(1 - \frac{C_t}{C_0}\right) \times 100 \quad (3)$$

where DL is the net degradation level percentage [%], and C_t and C_0 are the concentrations [ppb] of the PAH in the irradiated sample and original sample, respectively.

2.7. Quality assurance and quality control

All samples were spiked with the internal standard before chemical analysis to compensate for instrumental variations. Prior to sample extraction, the samples were spiked with the surrogate standard mixture to monitor net recovery levels. The measured recovery levels were within the acceptable range (80–120%) for the four surrogate standards (acenaphthene-d_{10}, phenanthrene-d_{10}, chrysene-d_{12}, and perylene-d_{12}), the lower recovery levels were for acenaphthene-d_{10} and phenanthrene-

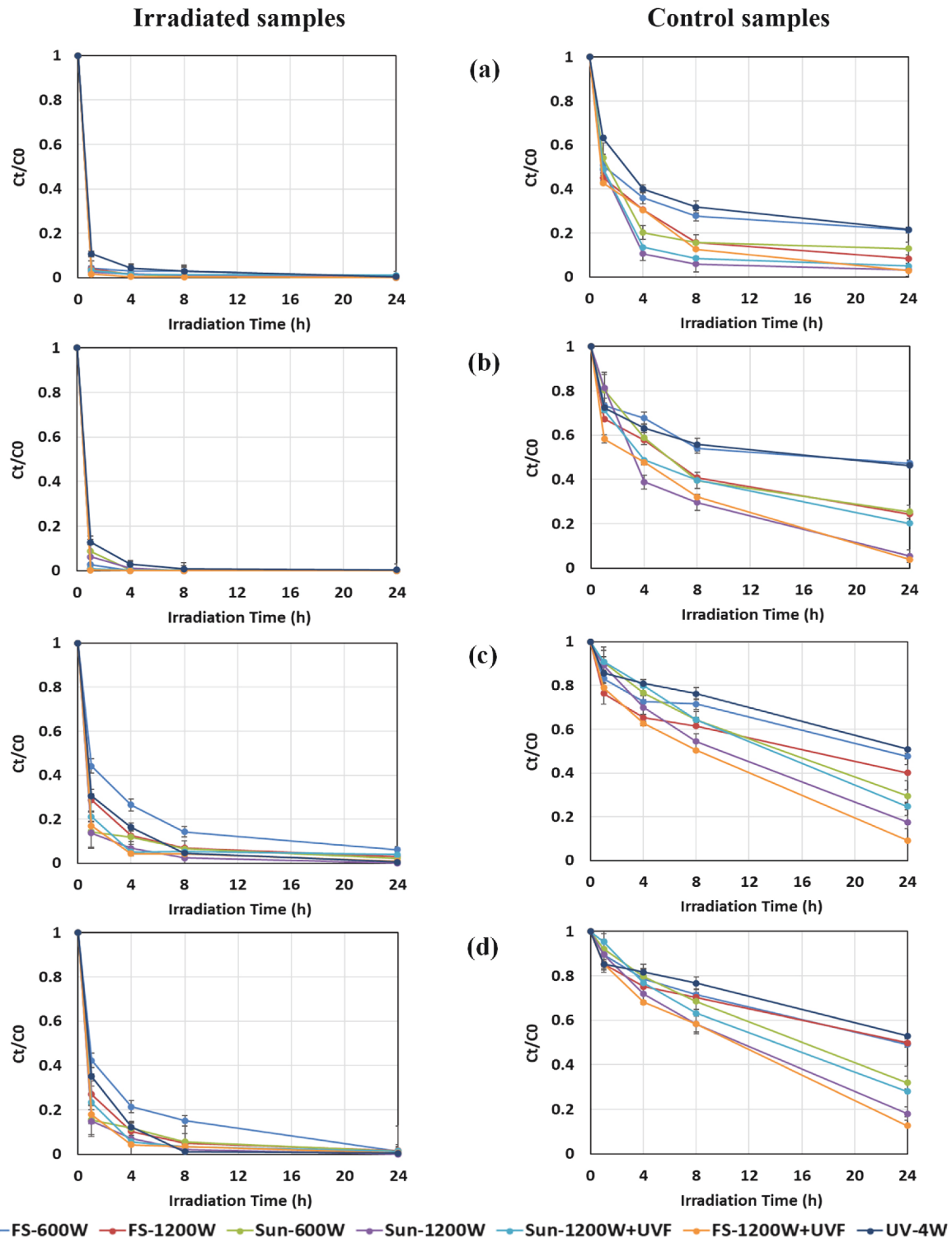

Fig. 3. Changes in the concentrations of MMW PAHs with irradiation time under full-spectrum LED light at two irradiance levels (FS–600 W and FS-1200W), sunlight during cloudy (Sun-600 W) and clear (Sun-1200 W) conditions, clear sunlight with a UV filter (Sun-1200 W+UVF), full-spectrum LED light with a UV filter (FS–1200 W+UVF), and UV-A LED light (UV–4W). a) phenanthrene, b) anthracene, c) fluoranthene, and d) pyrene. The initial concentration of the samples was 1000 ppb.

d_{10} (volatile PAHs) and the higher for chrysene-d_{12} and perylene-d_{12} (stable PAHs). A midpoint calibration standard (50 ppb or 100 ppb) was checked before starting a sample sequence to validate the instrument.

3. Results

The PAHs analyzed in this study are divided into three different categories based on their molecular weights. The categories include high molecular weight (HMW) PAHs (4–6 ring PAHs including benzo [*a*] anthracene, chrysene, benzo [*b*]fluoranthene, benzo [*k*]fluoranthene, benzo [*a*]pyrene, dibenz [*a,h*]anthracene, indeno [*1,2,3-cd*]pyrene, and benzo [*ghi*]perylene), medium molecular weight (MMW) PAHs (3–4 ring PAHs including phenanthrene, anthracene, fluoranthene, and pyrene), and low molecular weight (LMW) PAHs (2–3 ring PAHs including

Table 2
The first-order photodegradation rate constant (k) and net degradation level (DL) percentages of HMW PAHs degraded under various full-spectrum (FS) LED light and sunlight conditions. The initial concentration of the samples was 1000 ppb. Raw data are reported in Figs. 1 and 2.

HMW PAHs	k (h^{-1})				DL (%)			
	FS-600W	Sun-600 W	FS-1200W	Sun-1200 W	FS-600W	Sun-600 W	FS-1200W	Sun-1200 W
Benzo [*a*]anthracene	0.28	0.27	0.40	0.38	97	98	99	100
Chrysene	0.04	0.05	0.10	0.12	69	64	87	87
Benzo [*b*]fluoranthene	0.07	0.08	0.14	0.16	76	72	90	95
Benzo [*k*]fluoranthene	0.09	0.10	0.16	0.19	85	88	94	97
Benzo [*a*]pyrene	0.25	0.27	0.36	0.34	91	94	98	98
Dibenz [*a,h*]anthracene	0.11	0.12	0.19	0.20	84	86	94	95
Indeno [*1,2,3-cd*]pyrene	0.11	0.13	0.19	0.21	88	89	95	96
Benzo [*ghi*]perylene	0.09	0.10	0.14	0.17	82	85	92	95

naphthalene, acenaphthylene, acenaphthene, and fluorene). The sections below present the results of the irradiated and control samples for the 16 USEPA PAHs divided into three different categories (HMW, MMW, and LMW) for the samples exposed to two types of artificial LED lights (full-spectrum and UV-A) and natural sunlight.

The results of the full-spectrum LED light are reported at two different irradiance levels of 600 W/m^2 and 1200 W/m^2 defined as FS-600W and FS-1200W, respectively. The results under natural sunlight include two different outdoor conditions of cloudy (irradiance level of 600 W/m^2) and clear (irradiance level of 1200 W/m^2) defined as Sun-600 W and Sun-1200 W, respectively. The results of the UV-A LED light are reported at the irradiance level of 4 W/m^2 (UV–4W).

To further investigate the influence of UV wavelength on the photodegradation of PAHs, the UV wavelength from the full-spectrum LED light and natural sunlight was filtered out using the OP-3 UV filtering sheet. The effectiveness of the UV filter was tested by using it under the UV-A LED light and no degradation of HMW PAHs was observed, confirming that the OP-3 filter effectively filters out the entire UV-A range. UV filtering experiments were performed only under the highest irradiance level of 1200 W/m^2 for the full-spectrum LED light (FS–1200 W+UVF) and clear sunlight conditions (Sun-1200 W+UVF).

3.1. Fate of HMW PAHs

The concentration changes of HMW PAHs for the samples exposed to two different LED lights (full-spectrum and UV-A) and two different sunlight conditions (cloudy and clear) with and without the UV filter are shown for the initial concentrations of 1000 ppb in Figs. 1 and 2 and 100 ppb in Figs. S2 and S3. The results of HMW PAHs under all light sources show that the degradation of HMW PAHs is directly related to the photodegradation process for the initial concentrations of 1000 ppb PAHs (Figs. 1 and 2) and 100 ppb PAHs (Figs. S2 and S3), as the concentrations of the control samples remained constant suggesting evaporation is not a degradation pathway.

3.2. Fate of MMW PAHs

The concentration changes of MMW PAHs under the LED lights (full-spectrum and UV-A) and natural sunlight (cloudy and clear conditions) with and without the UV filter are presented for the initial concentrations of 1000 ppb in Fig. 3 and 100 ppb in Fig. S4. The results of MMW PAHs under all light sources indicate that the degradation of MMW PAHs is due to both photodegradation and evaporation processes for the initial concentrations of 1000 ppb PAHs (Fig. 3) and 100 ppb PAHs (Fig. S4), as the concentrations of all control samples decreased suggesting the evaporation process contributes to the degradation of MMW PAHs.

3.3. Fate of LMW PAHs

All LMW PAHs including naphthalene, acenaphthylene, acenaphthene, and fluorene in the samples with both initial concentrations of PAHs (100 ppb and 1000 ppb) degraded completely within 1 h in the irradiated and control samples under all light sources, which is expected since the LMW PAHs are highly volatile compounds. Complete removals of LMW PAHs in all control samples after 1 h indicate that the degradation of the LMW PAHs is fully controlled by the evaporation process and not the photodegradation process. Therefore, LMW PAHs are not discussed in this study to validate the hypotheses.

4. Discussion

4.1. Hypothesis 1: comparing the photodegradation patterns of PAHs under full-spectrum LED light and natural sunlight

The photodegradation patterns of HMW PAHs under the full-spectrum LED light (irradiance level of 600 W/m^2) are similar to the photodegradation patterns under cloudy conditions of natural sunlight (irradiance level of 600 W/m^2) at all time intervals (1, 4, 8, and 24 h) and for the initial concentrations of 1000 ppb PAHs (Figs. 1 and 2) and 100 ppb PAHs (Figs. S2 and S3). Similarly, the photodegradation patterns under the full-spectrum LED light with a higher irradiance level (1200 W/m^2) are similar to the photodegradation patterns under clear conditions of natural sunlight (irradiance level of 1200 W/m^2). The results suggest that the photodegradation of HMW PAHs scales to the irradiance levels of the light sources, and the full-spectrum LED light stimulates PAH photodegradation similar to natural sunlight.

The photodegradation rates of HMW PAHs follow a first-order kinetic reaction (Eq. (1)) with R^2 values of 0.95 or greater. The k values of each HMW PAH for the initial concentration of 1000 ppb PAHs (Table 2) are almost identical to the k values of 100 ppb PAHs (Table S4), the differences between the k values for each of the HMW PAHs range from 0 to 0.06 h^{-1}. The k values of HMW PAHs under the full-spectrum LED light are identical to the k values under natural sunlight for the same irradiance levels (the differences between the k values for each of the HMW PAHs range from 0 to 0.03 h^{-1}). As expected, the higher irradiance level (1200 W/m^2) yields higher photodegradation rates compared to the lower irradiance (600 W/m^2) for all HMW PAHs (see Table 2 and Table S4). The k values are roughly doubled for the irradiance level of 1200 W/m^2 compared to the irradiance level of 600 W/m^2. The results of the higher photodegradation rates for the higher irradiance levels of the lights are consistent with Marquès et al. (2016a) study that also observed higher photodegradation rates in coarse-textured soils exposed to PAHs when increasing the irradiance of fluorescent light (24 W/m^2 compared to 9.6 W/m^2). Also, Saeed et al. (2011) reported the higher light irradiance (750 W/m^2 compared to 250 and 500 W/m^2) had the greatest effect on photodegradation rates of PAHs in the water-soluble fraction of Kuwait crude oil exposed to UV-A xenon lamp.

The net degradation levels after 24 h of the full-spectrum LED light (1 full day indoor) are similar to the net degradation levels after 24 h of clear sunlight (3-days outdoor, considering 8 h sun/day) for all HMW PAHs in the samples with 1000 ppb PAHs (Table 2) and 100 ppb PAHs (Table S4) when comparing the same irradiance levels. The highest degradation percentages of HMW PAHs are for benzo [*a*]anthracene and

Table 3
The first-order photodegradation rate constants (k) and net degradation level (DL) percentages of HMW PAHs degraded under UV-A LED light and clear sunlight conditions. The initial concentration of the samples was 1000 ppb. Raw data are reported in Figs. 1 and 2.

HMW PAHs	k (h^{-1})		DL (%)	
	UV-4W	Sun-1200 W	UV-4W (after 8 h)	Sun-1200 W (after 24 h)
Benzo [*a*] anthracene	0.45	0.38	99	100
Chrysene	0.25	0.12	87	87
Benzo [*b*] fluoranthene	0.29	0.16	91	95
Benzo [*k*] fluoranthene	0.33	0.19	93	97
Benzo [*a*]pyrene	0.44	0.34	98	98
Dibenz [*a,h*] anthracene	0.33	0.20	94	95
Indeno [*1,2,3-cd*] pyrene	0.36	0.21	95	96
Benzo [*ghi*]perylene	0.30	0.17	92	95

Table 4
The normalized first-order photodegradation rate constant (k_n) of HMW PAHs degraded under various full-spectrum (FS) LED light, sunlight, and UV-A LED light. The initial concentration of the samples was 1000 ppb. Raw data are reported in Figs. 1 and 2 and 2.

HMW PAHs	k_n [h^{-1}/(kW/m^2)]				
	FS-600W	Sun-600 W	FS-1200W	Sun-1200 W	UV-4W
Benzo [*a*]anthracene	0.47	0.45	0.33	0.32	113
Chrysene	0.07	0.08	0.08	0.10	63
Benzo [*b*] fluoranthene	0.12	0.13	0.12	0.13	73
Benzo [*k*] fluoranthene	0.15	0.17	0.13	0.16	83
Benzo [*a*]pyrene	0.42	0.45	0.30	0.28	110
Dibenz [*a,h*] anthracene	0.18	0.20	0.16	0.17	83
Indeno [*1,2,3-cd*] pyrene	0.18	0.22	0.16	0.18	90
Benzo [*ghi*]perylene	0.15	0.17	0.12	0.14	75

benzo [*a*]pyrene with 98%–100% net degradation for 1200 W/m^2 irradiance level and 91%–100% for 600 W/m^2 irradiance level (see Table 2 and Table S4). The lowest degradation percentages are for chrysene, which range from 87% to 93% for 1200 W/m^2 irradiance level and 64%–72% for 600 W/m^2 irradiance level (see Table 2 and Table S4). Although benzo [*a*]anthracene and chrysene have the same molecular weights, benzo [*a*]anthracene is more sensitive to photodegradation compared to chrysene. These results are comparable with the results reported by John et al. (2016), which also observed more photodegradation percentages for benzo [*a*]anthracene compared to chrysene in DWH reference crude oil when the oil was exposed to sunlight.

The net degradation levels of MMW PAHs through evaporation in the control samples range from 74% to 100% for the initial concentrations of 100 ppb (Table S5) and 50%–97% for the initial concentrations of 1000 ppb (Table S6), with less removal associated with higher molecular weight PAHs. Photodegradation also contributes to the degradation process as the decrease in the concentrations of MMW PAHs is higher in the irradiated samples than in the control samples (see Fig. 3 and Fig. S4). After 24 h of the full-spectrum LED light and natural sunlight, all MMW PAHs are completely degraded from the irradiated samples (net degradation levels range between 95% and 100%) for the irradiance levels of 600 W/m^2 and 1200 W/m^2 and the initial concentrations of 100 ppb (Table S5) and 1000 ppb (Table S6). These results are consistent with Marquès et al. (2016b) study that also observed that evaporation contributed to the degradation of MMW PAHs, and photodegradation accelerated the entire degradation process, especially in fine-textured soils exposed to PAHs under a fluorescent light in a climate chamber when compared to control samples.

4.2. Hypothesis 2: comparing the photodegradation patterns of PAHs under the UV-A LED light, full-spectrum LED light, and natural sunlight

The photodegradation rates of HMW PAHs are higher under the UV-A LED light compared to the full-spectrum LED light and natural sunlight (see Figs. 1 and 2 and Figs. S2 and S3). The results of the UV-A LED light are mostly discussed and compared to the results of natural sunlight in this section, the comparison is the same for the full-spectrum LED light since the full-spectrum LED light stimulates PAH photodegradation similar to natural sunlight according to the previous section.

The net degradation levels after 8 h of the UV-A LED light are similar to the net degradation levels after 24 h of clear sunlight for all HMW PAHs in the initial concentrations of 1000 ppb (Table 3) and 100 ppb (Table S7), the differences between the net degradation for each of the HMW PAHs range from 0 to 5%. Therefore, the single-wavelength UV-A LED light (365 nm, irradiance of 4 W/m^2) accelerates the photodegradation rates of HMW PAHs compared to natural sunlight (irradiance of 1200 W/m^2).

Most of the PAH compounds absorb light in the UV range (Shankar et al., 2015), thus the higher photodegradation rates of HMW PAHs are observed under the UV-A LED light compared to natural sunlight (see Table 3 and Table S7 for the k values). Generally, a high photodegradation rate of PAHs under UV light has been previously observed. For example, Shao (2017) showed the photodegradation rates of three selected PAHs (phenanthrene, fluorene, and pyrene) in water were substantially fast in the presence of a 10 W low-pressure UV mercury lamp (254 nm) with the k values of 2.7, 1.86, and 1.02 h^{-1} for phenanthrene, fluorene, and pyrene, respectively. Clark et al. (2007) reported a very fast photodegradation rate for pyrene in water with the k value of 16.08 h^{-1} under a 200 W xenon/mercury UV light irradiation. Malloci et al. (2004) found that PAHs display $\pi^* \leftarrow \pi$ electronic transitions (strong excitation levels that help the photodegradation of PAHs) in the UV range rather than in visible and near IR. Our study compares the high photodegradation rates of PAHs under the UV-A LED light to the rates under natural sunlight and also the full-spectrum LED light, emphasizing the influence of a single-wavelength UV-A light compared to other light sources.

The UV-A LED light with a very low irradiance level of 4 W/m^2 can degrade the PAHs faster than the full-spectrum LED light and natural sunlight with an irradiance level of 1200 W/m^2. To better compare the photodegradation rates without the effect of light irradiances, the k values can be normalized to irradiance levels of the lights according to Eq. (2) (see Table 4 and Table S8). The normalized k_n values of the HMW PAHs under the full-spectrum LED light and natural sunlight are almost identical, the values for all HMW PAHs are less than 1 h^{-1}/(kW/m^2). However, the k_n values of HMW PAHs are considerably higher under the UV-A light, and the values for all HMW PAHs range from 53-115 h^{-1}/(kW/m^2). The k_n values are higher for the UV-A LED light because the denominator in Eq. (2), which is the light irradiance, is very smaller for the UV-A LED light (4 W/m^2) than the full-spectrum LED light and natural sunlight (1200 W/m^2). These results emphasize the influence of UV wavelength in the photodegradation of PAHs since the k_n values are almost 200–1000 times higher than the full-spectrum LED light and natural sunlight.

4.3. Additional validation data for hypothesis 2: photodegradation of PAHs under the UV-filtered natural sunlight and UV-filtered full-spectrum LED light

The photodegradation rates (k values) of HMW PAHs decrease under natural sunlight with clear conditions by using a UV filter (see Tables 2 and 5 for the initial concentrations of 1000 ppb and Tables S4 and S9 for

Table 5
The first-order photodegradation rate constants (k), normalized first-order photodegradation rate constant (k_n), and net degradation level (DL) percentages of HMW PAHs degraded under clear sunlight and full-spectrum (FS) LED light with a UV filter. The initial concentration of the samples was 1000 ppb. Raw data are reported in Figs. 1 and 2.

HMW PAHs	k (h^{-1})		k_n [h^{-1}/(kW/m^2)]		DL (%)	
	Sun-1200 W+UVF	FS-1200W+UVF	Sun-1200 W+UVF	FS-1200W+UVF	Sun-1200 W+UVF	FS-1200W+UVF
Benzo [*a*]anthracene	0.27	0.37	0.23	0.31	99	98
Chrysene	0.05	0.14	0.04	0.12	59	91
Benzo [*b*]fluoranthene	0.05	0.12	0.04	0.10	64	89
Benzo [*k*]fluoranthene	0.07	0.15	0.06	0.13	81	95
Benzo [*a*]pyrene	0.23	0.33	0.19	0.28	90	98
Dibenz [*a,h*]anthracene	0.08	0.16	0.07	0.13	86	96
Indeno [*1,2,3-cd*]pyrene	0.09	0.17	0.08	0.14	87	93
Benzo [*ghi*]perylene	0.07	0.13	0.06	0.11	76	94

the initial concentrations of 100 ppb). The photodegradation patterns observed after filtering UV light from clear sunlight conditions are similar to the photodegradation patterns observed for cloudy sunlight conditions without filtering UV light (see Figs. 1 and 2 and Figs. S2 and S3). These patterns suggest that filtering UV light from sunlight with clear conditions and a higher irradiance level (1200 W/m^2) behaves similarly to cloudy conditions with a lower irradiance level (600 W/m^2). The results also show that filtering UV light from natural sunlight decreases the photodegradation rates of HMW PAHs to half of the irradiance level. The k_n values are decreased by half for clear sunlight with the UV filter compared to the results without the UV filter (see Tables 4 and 5 and Tables S8 and S9), further confirming the importance of UV light for facilitating photodegradation.

The photodegradation patterns of HMW PAHs under the full-spectrum LED light by using a UV filter are similar to the photodegradation patterns without filtering UV light in the initial concentrations of 1000 ppb (Figs. 1 and 2) and 100 ppb (Figs. S2 and S3). Tables 4 and 5 for the initial concentrations of 1000 ppb and Tables S8 and S9 for the initial concentrations of 100 ppb also confirm that the k_n values are almost identical for the full-spectrum LED light with and without a UV filter. These results are expected since the full-spectrum LED light contains a very small range of UV light (380–400 nm), which is near the visible light and the UV filter had a negligible effect on this range. Table 5 and Table S9 show that the net degradation levels decrease more for clear sunlight with a UV filter as compared to the full-spectrum LED light with a UV filter.

5. Conclusions

The photodegradation rates of 16 USEPA PAHs were investigated using natural sunlight (under cloudy and clear conditions), and two types of artificial LED light sources (with full-spectrum and UV-A wavelengths) for two different initial concentrations of PAHs (100 ppb and 1000 ppb). The HMW PAHs data show that these compounds degrade primarily due to the photodegradation process. The MMW PAHs degrade due to both evaporation and photodegradation processes, while the LMW PAHs degrade rather rapidly via the evaporation process. The HMW PAHs photodegradation data follow first-order reaction kinetics, and the rate of the reaction depends on two factors: the amount of irradiation and the wavelength of the irradiation.

The results of this study validate the hypothesis that the full-spectrum LED-light-induced photodegradation rates of PAHs are similar to the natural sunlight-induced photodegradation rates when the rates are appropriately scaled to the irradiance levels. Therefore, PAH photodegradation studies that require sunlight can be conducted using the low-cost, full-spectrum LED light used in this study. The laboratory-scale setup avoids complex outdoor variabilities due to cloud cover, wind, dust, and rain.

Our results also show that UV wavelengths play a significant role in mediating the photodegradation process. This is expected because most of the PAH compounds absorb light in the UV range, which provides strong excitation for PAH photodegradation. The influence of UV radiation was tested in this study by using a filter to remove the UV range from all three light sources (sunlight, full-spectrum LED, and UV-A LED). The results show a significant decrease in the photodegradation rates for all HMW PAHs when the samples are exposed to sunlight. Since the full-spectrum LED light has very little radiation in the UV range (see Fig. S1), the difference in the rates with and without the UV filter is not significant. On the other hand, as expected, when the filter is used with the UV-A LED, the samples behaved like control samples with no photodegradation.

The UV-A LED light source experiments demonstrate that a UV light source with a single wavelength and low irradiance level of 4 W/m^2 can photodegrade the HMW PAHs at a much higher rate than natural sunlight and the full-spectrum LED. When normalized to the irradiance levels, the photodegradation rate constants of HMW PAHs using the UV-A light are about 200 to 1000 times higher than the rate constants obtained using sunlight and the full-spectrum LED light. Therefore, the UV-A LED light bulb is the most efficient and cost-effective light source for conducting laboratory-scale PAH photodegradation studies.

Author contribution statements

MA, TPC, and LT jointly conceived the ideas for this work. MA conducted experimental work, prepared figures, and wrote the manuscript. TPC and LT reviewed multiple versions of this manuscript and provided helpful comments. TPC and LT jointly supervised the work and developed the funding support and laboratory facilities.

Declaration of competing interest

The authors declare the following financial interests/personal relationships which may be considered as potential competing interests: Prabhakar Clement reports financial support was provided by National Science Foundation. Prabhakar Clement reports a relationship with National Science Foundation that includes: funding grants.

Data availability

Data will be made available on request.

Acknowledgments

This work was, in part, funded by the Center for Water Quality Research and the College of Engineering of the University of Alabama, and by a research grant awarded by the National Science Foundation (Award no: 2019561). We like to thank Environmental Research reviewers and Dr. Yuehan Lu for providing several thoughtful review comments. All three authors read and approved the final manuscript and their overall responsibilities, estimated using Clement (2014) approach, are MA (55%), LT (20%), and TPC (25%).

Appendix A. Supplementary data

Supplementary data to this article can be found online at https://doi.org/10.1016/j.envres.2022.114951.

References

Aeppli, C., 2022. Recent advance in understanding photooxidation of hydrocarbons after oil spills. Current Opinion in Chemical Engineering 36, 100763.

Arekhi, M., Terry, L.G., John, G.F., Al-Khayat, J.A., Castillo, A.B., Vethamony, P., Clement, T.P., 2020. Field and laboratory investigation of tarmat deposits found on Ras Rakan Island and northern beaches of Qatar. Sci. Total Environ. 735, 139516.

Chen, S.-J., Hsieh, L.-T., Chiu, S.-C., 2003. Emission of polycyclic aromatic hydrocarbons from animal carcass incinerators. Sci. Total Environ. 313 (1–3), 61–76.

Clark, C.D., De Bruyn, W.J., Ting, J., Scholle, W., 2007. Solution medium effects on the photochemical degradation of pyrene in water. J. Photochem. Photobiol. Chem. 186 (2–3), 342–348.

Clement, T.P., 2014. Authorship matrix: a rational approach to quantify individual contributions and responsibilities in multi-author scientific articles. Sci. Eng. Ethics 20 (2), 345–361.

Clement, T.P., John, G.F., 2022. A perspective on the state of Deepwater Horizon oil spill related tarball contamination and its impacts on Alabama beaches. Current Opinion in Chemical Engineering 36, 100799.

Dai, C., Han, Y., Duan, Y., Lai, X., Fu, R., Liu, S., Leong, K.H., Tu, Y., Zhou, L., 2022. Review on the contamination and remediation of polycyclic aromatic hydrocarbons (PAHs) in coastal soil and sediments. Environ. Res. 205, 112423.

Esen, V., Sağlam, Ş., Oral, B., 2017. Light sources of solar simulators for photovoltaic devices: a review. Renew. Sustain. Energy Rev. 77, 1240–1250.

Freeman, D.H., Ward, C.P., 2022. Sunlight-driven dissolution is a major fate of oil at sea. Sci. Adv. 8 (7), eabl7605.

Gupta, H., Gupta, B., 2015. Photocatalytic degradation of polycyclic aromatic hydrocarbon benzo [a] pyrene by iron oxides and identification of degradation products. Chemosphere 138, 924–931.

Gustitus, S.A., Clement, T.P., 2017. Formation, fate, and impacts of microscopic and macroscopic oil-sediment residues in nearshore marine environments: a critical review. Rev. Geophys. 55 (4), 1130–1157.

Han, Y., Yin, F., John, G.F., Clement, T.P., 2020. Understanding the relative performance of SCAN, SIM, PMRM and MRM methods for quantifying polycyclic aromatic hydrocarbons in crude oil samples. Rapid Commun. Mass Spectrom. 34 (11), e8765.

John, G.F., Han, Y., Clement, T.P., 2016. Weathering patterns of polycyclic aromatic hydrocarbons contained in submerged Deepwater Horizon oil spill residues when re-exposed to sunlight. Sci. Total Environ. 573, 189–202.

King, S.M., Leaf, P.A., Olson, A.C., Ray, P.Z., Tarr, M.A., 2014. Photolytic and photocatalytic degradation of surface oil from the Deepwater Horizon spill. Chemosphere 95, 415–422.

Li, W., Zhu, N., Shen, Y., Yuan, H., 2021. Towards efficient elimination of polycyclic aromatic hydrocarbons (PAHs) from waste activated sludge by ozonation. Environ. Res. 195, 110783.

Linden, K.J., Neal, W.R., Serreze, H.B., 2014. Adjustable Spectrum LED Solar Simulator. SPIE, pp. 109–117.

López-Fraguas, E., Sánchez-Pena, J.M., Vergaz, R., 2019. A low-cost LED-based solar simulator. IEEE Trans. Instrum. Meas. 68 (12), 4913–4923.

Malloci, G., Mulas, G., Joblin, C., 2004. Electronic absorption spectra of PAHs up to vacuum UV-Towards a detailed model of interstellar PAH photophysics. Astron. Astrophys. 426 (1), 105–117.

Mambwe, M., Kalebaila, K., Johnson, T., 2021. Remediation technologies for oil contaminated soil. Global Journal of Environmental Science and Management 7 (3), 419–438.

Marquès, M., Mari, M., Audí-Miró, C., Sierra, J., Soler, A., Nadal, M., Domingo, J.L., 2016a. Climate change impact on the PAH photodegradation in soils: characterization and metabolites identification. Environ. Int. 89, 155–165.

Marquès, M., Mari, M., Audí-Miró, C., Sierra, J., Soler, A., Nadal, M., Domingo, J.L., 2016b. Photodegradation of polycyclic aromatic hydrocarbons in soils under a climate change base scenario. Chemosphere 148, 495–503.

Marquès, M., Mari, M., Sierra, J., Nadal, M., Domingo, J.L., 2017. Solar radiation as a swift pathway for PAH photodegradation: a field study. Sci. Total Environ. 581, 530–540.

Pizzini, S., Giuliani, S., Polonia, A., Piazza, R., Bellucci, L.G., Gambaro, A., Gasperini, L., 2022. PAHs, PCBs, PBDEs, and OCPs Trapped and Remobilized in the Lake of Cavazzo (NE Italy) Sediments: Temporal Trends, Quality, and Sources in an Area Prone to Anthropogenic and Natural Stressors. Environmental Research, 113573.

Radović, J.R., Aeppli, C., Nelson, R.K., Jimenez, N., Reddy, C.M., Bayona, J.M., Albaigés, J., 2014. Assessment of photochemical processes in marine oil spill fingerprinting. Mar. Pollut. Bull. 79 (1–2), 268–277.

Saeed, T., Ali, L.N., Al-Bloushi, A., Al-Hashash, H., Al-Bahloul, M., Al-Khabbaz, A., Al-Khayat, A., 2011. Effect of environmental factors on photodegradation of polycyclic aromatic hydrocarbons (PAHs) in the water-soluble fraction of Kuwait crude oil in seawater. Mar. Environ. Res. 72 (3), 143–150.

Shankar, R., Shim, W.J., An, J.G., Yim, U.H., 2015. A practical review on photooxidation of crude oil: laboratory lamp setup and factors affecting it. Water Res. 68, 304–315.

Shao, W.a., 2017. Study of kinetics mechanism of PAHs photodegradation in solution. Procedia Earth and Planetary Science 17, 348–351.

Sharpless, C., Aeppli, C., Reddy, C.M., Swarthout, B., Stewart, O.C., Walters, M., Valentine, D.L., 2016. Comparison of Experimenal Photooxidation Rates and Patterns in Glass-And Water-Based Oil Slicks with Daily Weathering Observed in the Gulf of Mexico. American Geophysical Union, 2016.

Song, K., Mohseni, M., Taghipour, F., 2016. Application of ultraviolet light-emitting diodes (UV-LEDs) for water disinfection: a review. Water Res. 94, 341–349.

Subramanian, G., Prakash, H., 2021. Photo augmented copper-based Fenton disinfection under visible LED light and natural sunlight irradiation. Water Res. 190, 116719.

Tavakoli, M., Jahantigh, F., Zarookian, H., 2021. Adjustable high-power-LED solar simulator with extended spectrum in UV region. Sol. Energy 220, 1130–1136.

Ullah, S., Khan, A.A., Jan, A., Aain, S.Q., Neto, E.P., Serge-Correales, Y.E., Parveen, R., Wender, H., Rodrigues-Filho, U.P., Ribeiro, S.J., 2020. Enhanced photoactivity of BiVO4/Ag/Ag2O Z-scheme photocatalyst for efficient environmental remediation under natural sunlight and low-cost LED illumination. Colloids Surf. A Physicochem. Eng. Asp. 600, 124946.

Vela, N., Martínez-Menchón, M., Navarro, G., Pérez-Lucas, G., Navarro, S., 2012. Removal of polycyclic aromatic hydrocarbons (PAHs) from groundwater by heterogeneous photocatalysis under natural sunlight. J. Photochem. Photobiol. Chem. 232, 32–40.

Yang, X., Cai, H., Bao, M., Yu, J., Lu, J., Li, Y., 2018. Insight into the highly efficient degradation of PAHs in water over graphene oxide/Ag3PO4 composites under visible light irradiation. Chem. Eng. J. 334, 355–376.

Yu, J., Gao, Y., Jiang, S., Sun, F., 2019. Naphthalimide aryl sulfide derivative norrish type I photoinitiators with excellent stability to sunlight under near-UV LED. Macromolecules 52 (4), 1707–1717.

Zhang, L.-h., Li, P.-j., Gong, Z.-q., Oni, A.A., 2006. Photochemical behavior of benzo [a] pyrene on soil surfaces under UV light irradiation. J. Environ. Sci. 18 (6), 1226–1232.

Zhang, L., Li, P., Gong, Z., Li, X., 2008. Photocatalytic degradation of polycyclic aromatic hydrocarbons on soil surfaces using TiO2 under UV light. J. Hazard Mater. 158 (2–3), 478–484.

Zhang, L., Xu, C., Chen, Z., Li, X., Li, P., 2010. Photodegradation of pyrene on soil surfaces under UV light irradiation. J. Hazard Mater. 173 (1–3), 168–172.